JCB Article

RhoA/ROCK regulation of neuritogenesis via profilin IIa–mediated control of actin stability

Jorge Santos Da Silva,[1] Miguel Medina,[1] Cecilia Zuliani,[2] Alessia Di Nardo,[3] Walter Witke,[3] and Carlos G. Dotti[1]

[1]Cavalieri Ottolenghi Scientific Institute, University of Turin, 10043 Orbassano, Torino, Italy
[2]Tumour Immunology Programme, German Cancer Research Centre, 69120 Heidelberg, Germany
[3]European Moleular Biology Laboratory, Mouse Biology Programme, 00016 Monterotondo, Italy

Neuritogenesis, the first step of neuronal differentiation, takes place as nascent neurites bud from the immediate postmitotic neuronal soma. Little is known about the mechanisms underlying the dramatic morphological changes that characterize this event. Here, we show that RhoA activity plays a decisive role during neuritogenesis of cultured hippocampal neurons by recruiting and activating its specific kinase ROCK, which, in turn, complexes with profilin IIa. We establish that this previously uncharacterized brain-specific actin-binding protein controls neurite sprouting by modifying actin stability, a function regulated by ROCK-mediated phosphorylation. Furthermore, we determine that this novel cascade is switched on or off by physiological stimuli. We propose that RhoA/ROCK/PIIa-mediated regulation of actin stability, shown to be essential for neuritogenesis, may constitute a central mechanism throughout neuronal differentiation.

Introduction

Neuritogenesis, the first step of neuronal differentiation, is characterized by breakage of the initial, approximately spherical symmetry as nascent neurites emerge from the soma (Da Silva and Dotti, 2002). These processes extend steadily until one (the future axon) starts growing more rapidly, inducing morphological polarization. As neurites extend further and acquire their final axonal or dendritic identities, neurons establish synaptic contacts and reach full maturation.

Different in vivo and in vitro studies over the last 30 yr have hinted at the importance of neuritogenesis. As neurons start migrating in the developing brain, they form new leading edges that develop into short extensions and operate as guides for migration (Hatten, 1999). Such extensions sprout as the early neurons contact particular extracellular environments (Baum and Garriga, 1997), and failure to do so precludes proper migration (Gleeson and Walsh, 2000). Thus, neuritogenesis is fundamental for initiating migration and patterning and, ultimately, for the inception of neuronal differentiation.

The intracellular events triggering neurite sprouting are not established. However, regulation of actin dynamics via particular signaling pathways is known to be a crucial mechanism directing the dramatic morphological changes observed in subsequent differentiation stages (Luo, 2002). One such group of actin-regulating pathways is directed by Rho small GTPases, such as RhoA (Luo, 2000). Overexpression of constitutively active RhoA has been shown to induce neurite retraction and arrest growth in neuronal cell lines (Jalink et al., 1993; Kozma et al., 1997) and in primary neuronal populations (Bito et al., 2000). Conversely, direct inactivation of RhoA by ADP-ribosylation (Sekine et al., 1989) using the C3-exoenzyme (a specific RhoA inhibitor) enhances neurite extension and growth cone movement (Jalink et al., 1994; Hirose et al., 1998). Likewise, inactivation of the RhoA kinase ROCK (a well-characterized downstream effector of RhoA) produces a similar effect in cerebellar granule cells (Bito et al., 2000). These findings suggest that the capacity of RhoA-directed pathways to control actin stability is fundamental to events such as neurite elongation, guidance, and branching.

Despite the fact that RhoA can convey information to the actin cytoskeleton during these developmental steps via cofilin

Address correspondence to Carlos G. Dotti, Cavalieri Ottolenghi Scientific Institute, University of Turin, via Regione Gonzole 10, 10043 Orbassano, Torino, Italy. Tel.: 390116708180. Fax.: 390116708149. email: carlos.dotti@unito.it

Key words: neuronal differentiation; hippocampal neurons; actin dynamics; Rho GTPases; actin-binding proteins

Abbreviations used in this paper: BDNF, brain-derived neurotrophic factor; HA-C3, HA-tagged Rho inhibitory toxin C3; NT-3, neurotrophin 3.

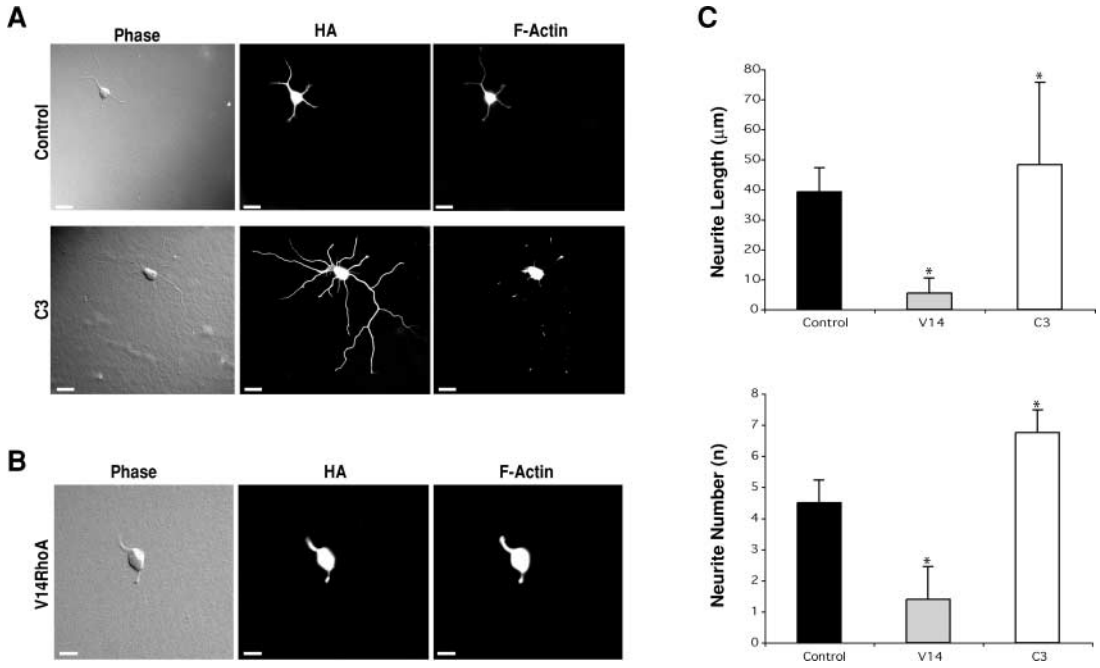

Figure 1. **RhoA negatively regulates neuritogenesis.** (A) Compared with cells transfected with a null HA plasmid (Control), RhoA inactivation (C3, 24 h) induces increased neurite sprouting and reduction of F-actin content. (B) Conversely, transfection of HA-tagged, constitutively active RhoA (V14RhoA) decreases neurite sprouting and increases accumulation of F-actin. (C) Quantitative comparison indicates that V14 ($n = 22$) decreases neurite length and number, compared with control cells (Control, $n = 35$), whereas C3 transfection ($n = 22$) increases process sprouting and elongation. Data are mean + SD values. *, $P < 0.001$, in comparison with control. Bars, 10 μm.

(Bamburg, 1999), other actin-binding proteins, such as the profilins, may be involved as well. Profilins have been implicated in the maintenance of cytoskeletal integrity in a variety of organisms such as *Dictyostelium discoideum* (Haugwitz et al., 1994), yeast (Haarer et al., 1990), and *Drosophila melanogaster* (Verheyen and Cooley, 1994). In the fly, the sole form of profilin (*chickadee*) has been shown to play a role in motor neuron axon extension as *chickadee* mutations arrest growth (Wills et al., 1999). In mammals, there are different profilin isoforms that, while sharing similar biochemical properties, have diverse tissue distributions. Profilin I (PI) is ubiquitous, whereas both profilin II isoforms (PIIa and PIIb) are largely restricted to the brain (Witke et al., 2001). A third profilin has been described recently and its expression detected exclusively in kidney and testis (Hu et al., 2001). Apart from the fact that PIIa is a brain-specific profilin isoform, the only actin-binding protein specifically interacting with the RhoA downstream kinase ROCK in brain extracts is PIIa (Witke et al., 1998). This led us to hypothesize that PIIa may be a key player in neuronal-specific events directed by the RhoA–ROCK pathway.

In this work, we show that RhoA and its specific downstream effector ROCK are essential during neuritogenesis in mammalian hippocampal neurons by modulating actin stability. Consistent with the aforementioned hypothesis, such modulation is dependent on the downstream effector profilin IIa, a protein of previously undetermined function. Furthermore, we show that this early neuronal program is regulated by different physiological stimuli. These findings reveal a central regulatory mechanism directing the, as yet, uncharacterized process of initial neuronal symmetry breakage.

Results

RhoA/ROCK negatively regulate neuritogenesis

To analyze the role of RhoA in neurite formation we performed loss- and gain-of-function experiments in cultured rat embryo hippocampal neurons, for which the sequence of postmitotic events is well described (Dotti et al., 1988).

We first determined the effect of expressing the HA-tagged Rho inhibitory toxin C3 (HA-C3). RhoA inactivation induces neurons to sprout more processes that extend further, when compared with mock-transfected control cells (Fig. 1 A). Next, we transfected neurons with a constitutively active version of RhoA (HA-V14RhoA). In this case, RhoA activation arrests cells in the round cell phase (Fig. 1 B). Consistent with the importance of actin instability for later events, such as axon elongation (Bradke and Dotti, 1999), cells that sprout more neurites upon RhoA inactivation have less filamentous actin (Fig. 1 A), whereas the opposite occurs in V14RhoA overexpressing cells (Fig. 1 B). Comparative statistical analysis (Fig. 1 C) illustrates the differences between mock-transfected controls and transfected cells, in terms of the number and length of nascent neurites. Given that, at later stages, RhoA activation also arrests differentiation whereas inactivation enhances it (Introduction), our results highlight that RhoA induces the same type of subcellular changes, irrespective of the time of development at which it is activated.

Next, we asked which downstream effectors of RhoA might relay signals that trigger neuritogenesis. RhoA has different effectors (Kaibuchi et al., 1999), but the most relevant to neuronal morphogenesis is the RhoA kinase or p160/ROCK (Nakagawa et al., 1996). ROCK inhibition pre-

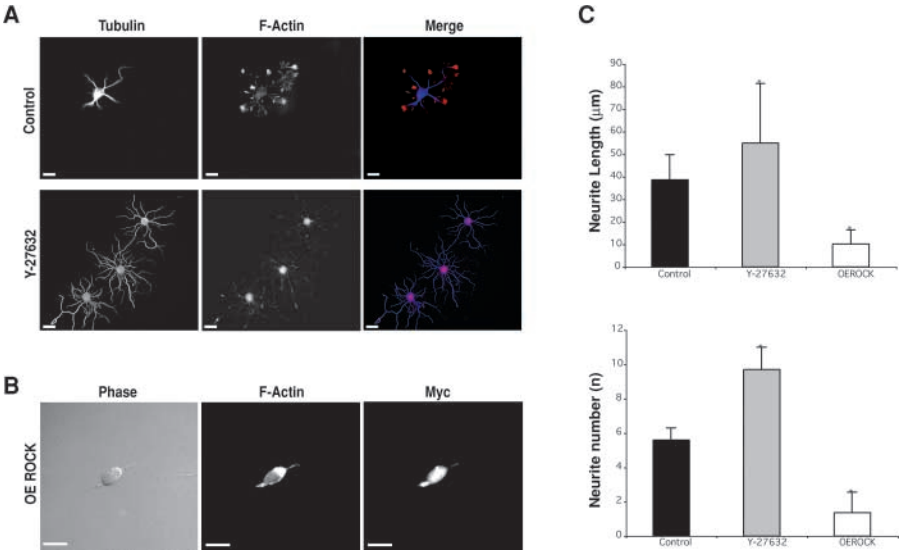

Figure 2. **RhoA kinase ROCK activity modulates neuritogenesis.** (A) ROCK inhibition (Y-27632, 18 h) induces multiple neurite sprouting and reduction of F-actin content, when compared with PBS buffer-treated controls. (B) In contrast, overexpression of myc-tagged ROCK (OE ROCK) severely inhibits neurite budding, and favors increased F-actin accumulation. (C) Quantitative analysis indicates that Y-27632–treated cells ($n = 29$) significantly sprout more and longer processes than control cells ($n = 25$), and that ROCK overexpression (OE ROCK, $n = 27$) severely reduces neurite sprouting and extension. Data are mean + SD values. *, $P < 0.001$, in comparison with control. Bars, 10 μm.

cludes RhoA-induced neurite retraction (Nakagawa et al., 1996; Hirose et al., 1998; Bito et al., 2000), and its activation leads to axonal (Billuart et al., 2001) and dendritic (Nakayama et al., 2000) retraction in mature neurons. These important findings indicate that, after axons and dendrites are committed, ROCK and its activity are necessary and largely sufficient to mediate RhoA-induced effects. Thus, we tested if loss of ROCK activity induces sprouting in immature neurons. Indeed, incubation of recently dissociated neurons with Y-237632 (a specific inhibitor of ROCK kinases; Ishizaki et al., 2000) induces the appearance of multiple neurites with increased length (Fig. 2 A) as compared with buffer-treated cells. As with RhoA inactivation, ROCK-inhibited cells show a marked reduction in F-actin. Conversely, ROCK overexpression induces an arrest in differentiation and, consistently, an intense F-actin staining is observed (Fig. 2 B). This phenotype is in all ways similar to that generated by overexpressing constitutively active RhoA, suggesting that the intracellular levels of the RhoA-specific kinase are essential for its overall activity. Statistical analysis highlights how modifying ROCK activity affects neuronal morphology, both in terms of neurite number and extent (Fig. 2 C), reflecting the similarities with what is observed when RhoA activity is modified (Fig. 1). Overall, these results indicate that the activities of RhoA and ROCK are essential to regulate actin stability and neurite sprouting in mammalian neurons.

PIIa is a negative regulator of neurite sprouting and elongation

ROCK is known to activate LIMK-1 (Maekawa et al., 1999), which, in turn, inhibits the actin-binding protein cofilin (Arber et al., 1998). This could be the pathway inducing the phenotypes described in RhoA/ROCK negatively regulate neuritogenesis. However, ROCK also binds the brain-specific actin-binding protein PIIa (Witke et al., 1998). This implies that for neuron-specific events the involvement of this actin regulatory protein may be critical. Moreover, the role of PIIa in mammalian neurons is not known. Therefore, we took a two-step approach: on the one hand, we analyzed the role of PIIa in hippocampal neuron neuritogenesis; and on the other hand, we investigated its dependence on the RhoA–ROCK pathway.

To determine the function of PIIa in early neuronal differentiation, we performed a loss-of-function analysis. We determined the effect of constitutive PIIa suppression by examining the phenotype of neurons derived from PII-deficient mice (unpublished data). Specific lack of PII expression in these cells was confirmed by Western blot analysis (Fig. 3 A). When compared with control PII+/− cells, PII-deficient cells display an increased number of highly branched budding neurites, with higher mean lengths (Fig. 3, A and C). These initial observations indicate that PIIa may be playing a critical role as a neurite sprouting regulator. However, at later times after seeding, the morphological differences between homozygous and heterozygous cells recede (unpublished data), probably due to homeostatic compensation. Thus, we suppressed PIIa expression using an effective antisense technique based on morpholino oligonucleotides (Summerton et al., 1997). With this approach, PIIa expression is reduced by 70% (ASPIIa), whereas the addition of missense oligonucleotides (misASPIIa) leaves PIIa levels unchanged (Fig. 3 B). Controls with the unrelated Golgi protein mannosidase-2 and with the related PI isoform confirm the specificity of the antisense method. Morphological analysis shows that ASPIIa cells have a higher number of sprouting neurites that are longer compared with misASPIIa cells. In addition, there is increased branching of neurites creating a complex neuritic tree, which is atypical at these early times in culture. Interestingly, analysis of neurite number and length reveals an analogous trend in both loss-of-function approaches (Fig. 3 C): although ASPIIa cells extend longer, more branched processes than PII −/− cells, their respective controls have a very similar average neurite extent. This confirms that acute reduction of PIIa accurately reproduces the phenotype induced by chronic gene deletion and that the severity of the effect is amplified.

Next, we asked if the opposite phenotype would be observed in gain-of-function conditions. We transfected hip-

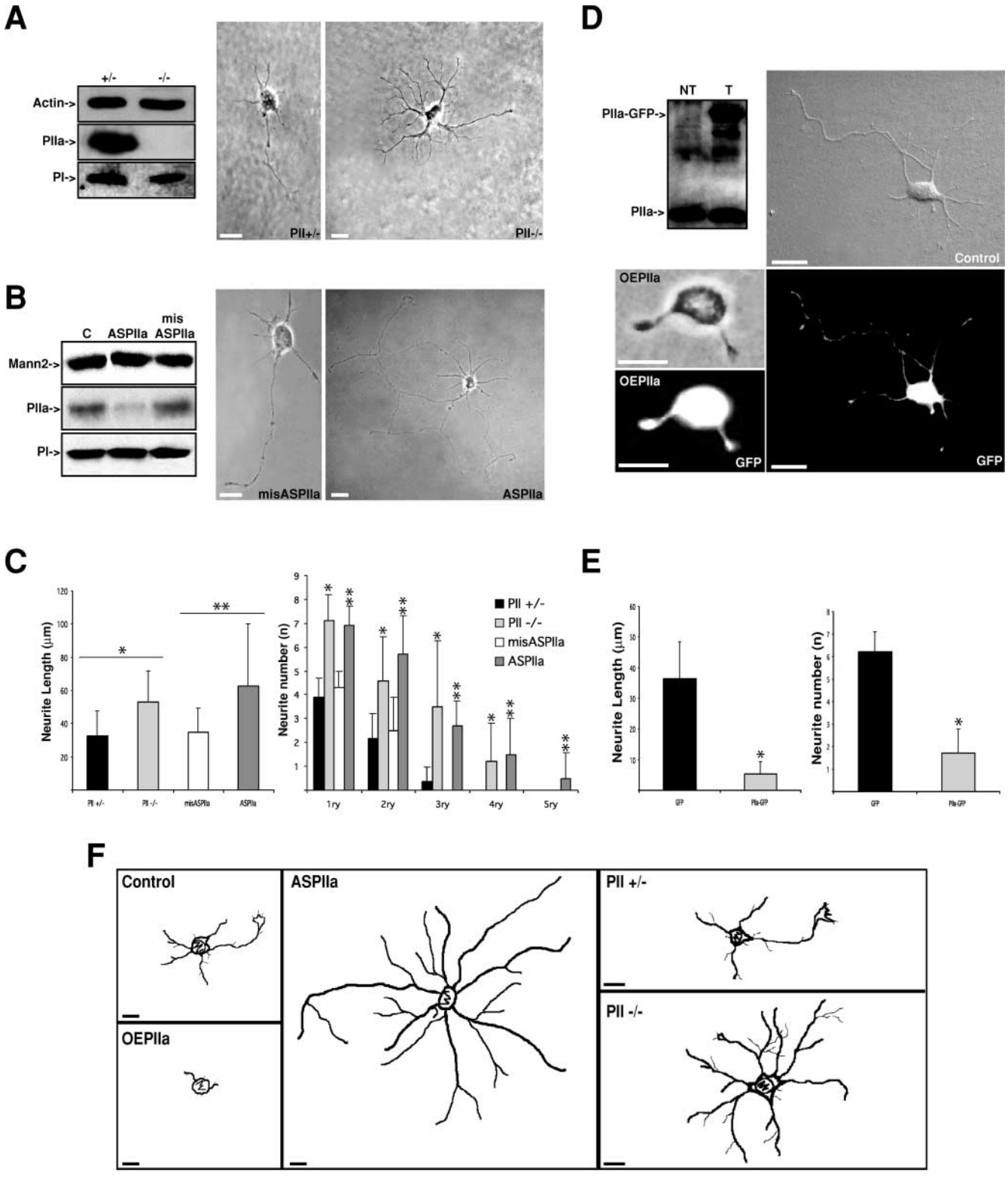

Figure 3. **PIIa is a negative regulator of neurite sprouting.** (A) Western blot of heterozygous (+/−) and PIIa-null mice (−/−) brain lysates probed for actin, PIIa, and PI showing that only PIIa expression is affected in PII−/− mice. Compared with PII+/− neurons, at 24 h, PII−/− cells exhibit multiple sprouting neurites with increased lengths. (B) PIIa-morpholino antisense oligonucleotides (ASPIIa) reduce PIIa levels by 70% in rat hippocampal neurons in culture, whereas PIIa-missense oligonucleotides (misASPIIa) do not alter PIIa expression, compared with untreated control cells (C). The unrelated Golgi protein mannosidase-2 (Mann2) and the closely related PI are unaffected by antisense treatment. At 24 h, misASPIIa neurons present a typical morphology, whereas ASPIIa cells display increased number of sprouting neurites and extreme elongation of most processes. (C) Quantitative analysis shows that mouse PII+/− and rat misASPIIa neurons display similar neurite number and length averages. PII−/− cells have a clear increase in the number, branching (up to quaternary, 4ry), and length of emergent processes (*, $P < 0.001$, PII−/− in comparison with PII+/−; PII+/−, $n = 23$; PII−/−, $n = 21$). Similarly, but more strikingly, ASPIIa rat hippocampal neurons exhibit increased neurite number, branching (up to quintenary, 5ry), and length when compared with misASPIIa cells

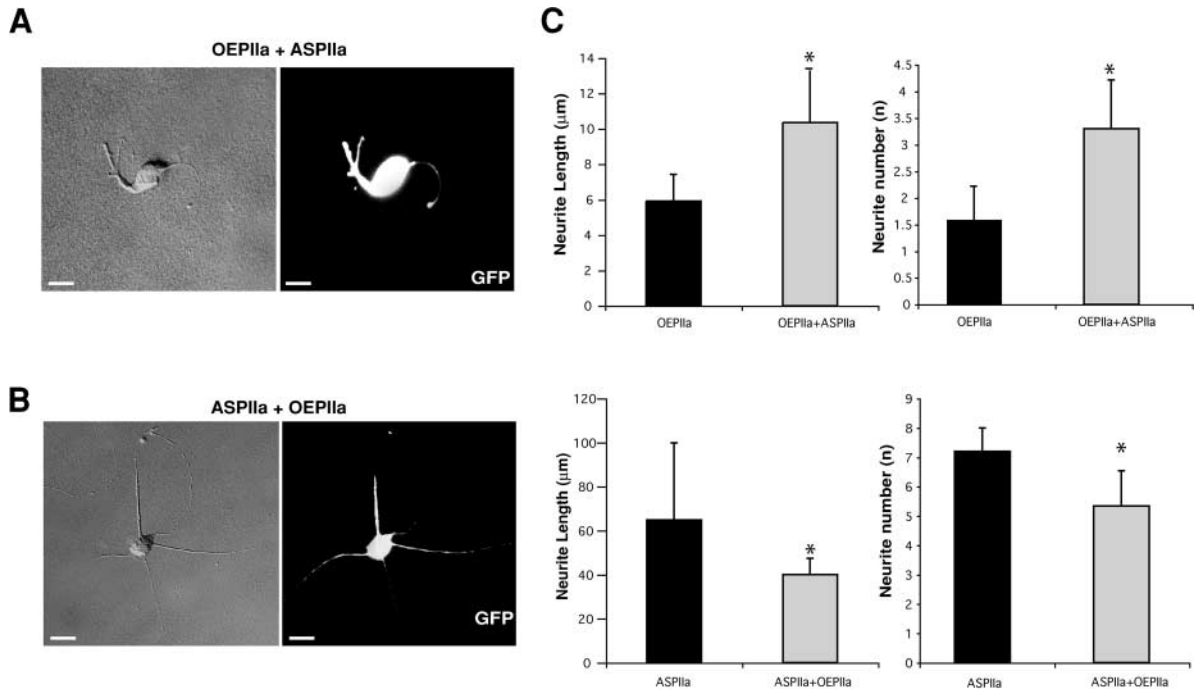

Figure 4. **The effects caused by PIIa loss- and gain-of-function approaches are reversible.** (A) PIIa overexpressing cells treated with PIIa antisense oligonucleotides (OEPIIa + ASPIIa) have more and longer neurites than overexpressing neurons only. (B) Expression of PIIa-GFP in a PIIa-antisense background (ASPIIa + OEPIIa) prevents the increase in neurite number and extension produced by severe PIIa reduction. (C) Quantitative analysis shows that both the gain- (OEPIIa) and loss-of-function (ASPIIa) phenotypes can be reciprocally and significantly rescued, in nascent neurite number and length. Data are mean + SD values. *, $P < 0.001$ for each pair; OEPIIa, $n = 19$; OEPIIa + ASPIIa, $n = 19$; ASPIIa, $n = 30$; ASPIIa + OEPIIa, $n = 22$. Bars, 10 μm.

pocampal neurons with a PIIa-GFP fusion construct, resulting in the detectable expression of the tagged protein (Fig. 3 D). PIIa-GFP expression produces cells with greatly reduced neurite number and length, in contrast with cells transfected with the equivalent GFP-null vector (Fig. 3, D and E). The same phenotype was observed with a construct containing a smaller epitope tag derived from Sendai virus and with an untagged PIIa vector (unpublished data). This ensures that the GFP moiety did not affect PIIa activity as expected because this construct has the ability to bind actin, without influence of the tag on the dynamics of polymerization (Di Nardo et al., 2000). Differences between the loss- and gain-of-function phenotypes are illustrated by camera lucida morphological reconstructions (see Materials and methods; Fig. 3 F). Our findings indicate that the intracellular availability of this 1:1 actin monomer-binding protein is essential for controlled neurite sprouting and suggest a novel role of PIIa as a key regulator of neuritogenesis.

To demonstrate the specificity of our loss- and gain-of-function approaches and to determine how direct the role of PIIa is in the sprouting and elongation of neurites, we performed phenotypic rescue experiments. Specifically, on a PIIa-GFP overexpression background we induced PIIa reduction (Fig. 4 A), and on PIIa antisense-treated cells we transiently transfected PIIa-GFP (Fig. 4 B). Statistical analysis (Fig. 4 C) reveals that both phenotypes can be reciprocally rescued in neurite number and length. This indicates that the morphological modifications induced by loss- or gain-of-function of PIIa are highly specific to this protein.

PIIa exerts its function by regulating the actin cytoskeleton

The effects of PIIa function are probably due to the capacity of this protein to influence actin stability. We tested this assumption by analyzing the levels of polymerized (filamentous) and monomeric (globular) actin, in the above loss- and gain-of-function models (see Materials and methods). Immunofluorescence analysis (Fig. 5 A) shows that, compared with control cells, the F-actin content of antisense-treated cells is markedly lower, whereas G-actin levels are higher. The opposite is observed for PIIa overexpressing cells. Determination of F- and G-actin contents (Fig. 5 A, histogram) reveals that PIIa antisense treatment induces a shift of the F/G-actin ratio from 1.33 in control cells to 0.71. Conversely, in PIIa overexpressing cells the F/G-actin ratio is shifted from 1.33 to 2.35. Because the level of G-actin in overex-

(**, $P < 0.001$, ASPIIa in comparison with misASPIIa; misASPIIa, $n = 26$; ASPIIa, $n = 25$). Data are mean + SD values. (D) Western blot shows detectable levels of PIIa-GFP in transfected (T) versus untransfected cells (NT). Overexpression of PIIa-GFP (OEPIIa) leads to differentiation arrest, at 24 h, when compared with GFP-only transfected neurons (Control). (E) Comparative analysis shows that transfection of PIIa-GFP induces a clear decrease in neurite budding and extension when compared with the mock GFP transfection. Data are mean + SD values. *, $P < 0.001$; GFP, $n = 35$; PIIa-GFP, $n = 31$. (F) Reconstruction of observed phenotypes illustrates the morphologies induced by PIIa loss and gain of function. Bars, 10 μm.

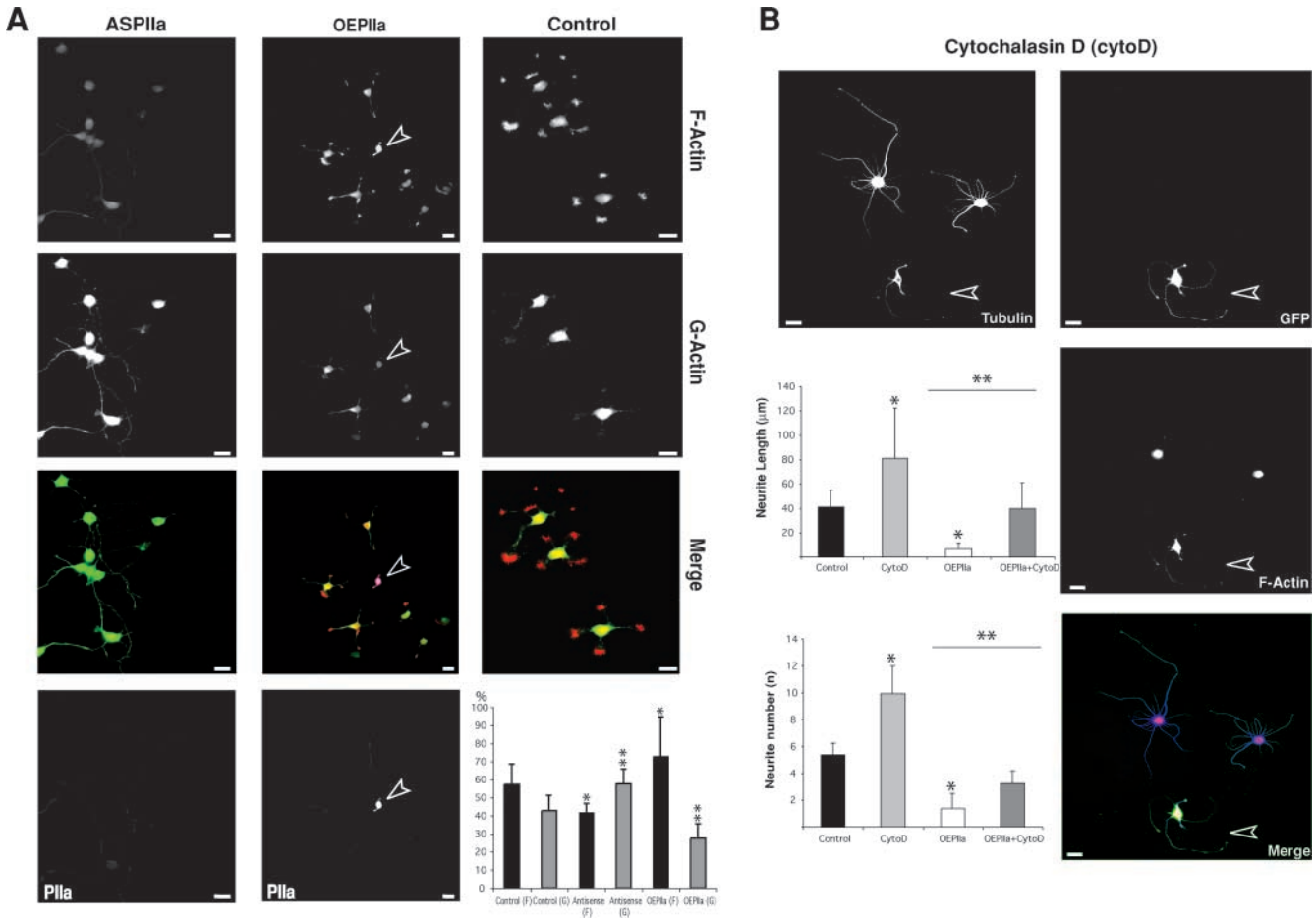

Figure 5. **PIIa modulates actin dynamics in early neuronal differentiation.** (A) Compared with buffer-treated (Control) neurons, antisense-treated cells display a generalized reduction of PIIa labeling along with lower F-actin fluorescence and higher G-actin levels. Overexpression of untagged PIIa (arrowhead) leads to increased F-actin content and decreased G-actin levels. Measurement of F- and G-actin indicates that, compared with the steady state, PIIa antisense increases the G-actin content, whereas OEPIIa cells have significantly more F-actin. Data are mean + SD values. *, $P < 0.001$, in comparison with control F-actin; **, $P < 0.001$, in comparison with control G-actin. (B) Untransfected cells are cytochalasin-D (cytoD) sensitive, sprouting numerous neurites with long, curled appearance. PIIa overexpressing cells (GFP positive, arrowhead) have higher cytoD resistance. Still, cytoD partially rescues the PIIa overexpression phenotype (compare with A). Cell measurements show that cytoD induces process sprouting and extension (cytoD, $n = 32$; control, $n = 35$) and that the OEPIIa phenotype ($n = 26$) is significantly reverted by cytoD-induced depolymerization of F-actin (OEPIIa + CytoD, $n = 22$). Data are mean + SD values. *, $P < 0.001$, in comparison with control; **, $P < 0.001$, OEPIIa in comparison with OEPIIa + CytoD. Bars, 10 μm.

pressing cells is much lower than in control cells and the F/G-actin ratio is significantly shifted toward the polymerized form, these results imply that increased levels of PIIa induce rapid re-addition of monomers to actin polymers (Selden et al., 1999; Wolven et al., 2000). These results, and the reciprocal reversibility of our loss- and gain-of-function approaches (Fig. 4), favor the possibility that changes in the F/G-actin ratio observed with overexpression or antisense of PIIa, are due to specific PIIa-mediated actin stabilization or destabilization rather than a simple change of the overall profilin/actin ratio.

To test this directly, we treated overexpressing neurons with cytochalasin D, which efficiently depolymerizes actin in cultured hippocampal neurons (Bradke and Dotti, 1999). Compared with untreated cells, cytochalasin D–treated neurons exhibit higher neurite number and length. Similarly, PIIa-GFP–transfected cells, otherwise arrested early in their differentiation program, show a phenotypic reversion to control-like levels, in both process length and number, upon cytochalasin D addition. Consistently, the F-actin content in these cells, although reduced in comparison with nontreated, overexpressing cells (Fig. 5 A, OEPIIa and histogram), is higher than that of neighboring untransfected cells (Fig. 5 B). Therefore, we can conclude that increased actin stability, due to higher F-actin content caused by PIIa overexpression, impedes sprouting and extension, whereas the extreme reduction of polymerized actin observed in PIIa antisense-treated cells, is probably the reason why neurites in these cells are more numerous and longer. Together, these observations substantiate the concept of PIIa regulation of neurite budding via control of actin stability.

ROCK interacts physically and functionally with PIIa

That ROCK and PIIa loss- and gain-of-function models generate similar phenotypes and both proteins coexist in a molecular complex (Witke et al., 1998) indicates that ROCK and PIIa could be working in tandem during neuritogenesis. To test this, we performed a series of bio-

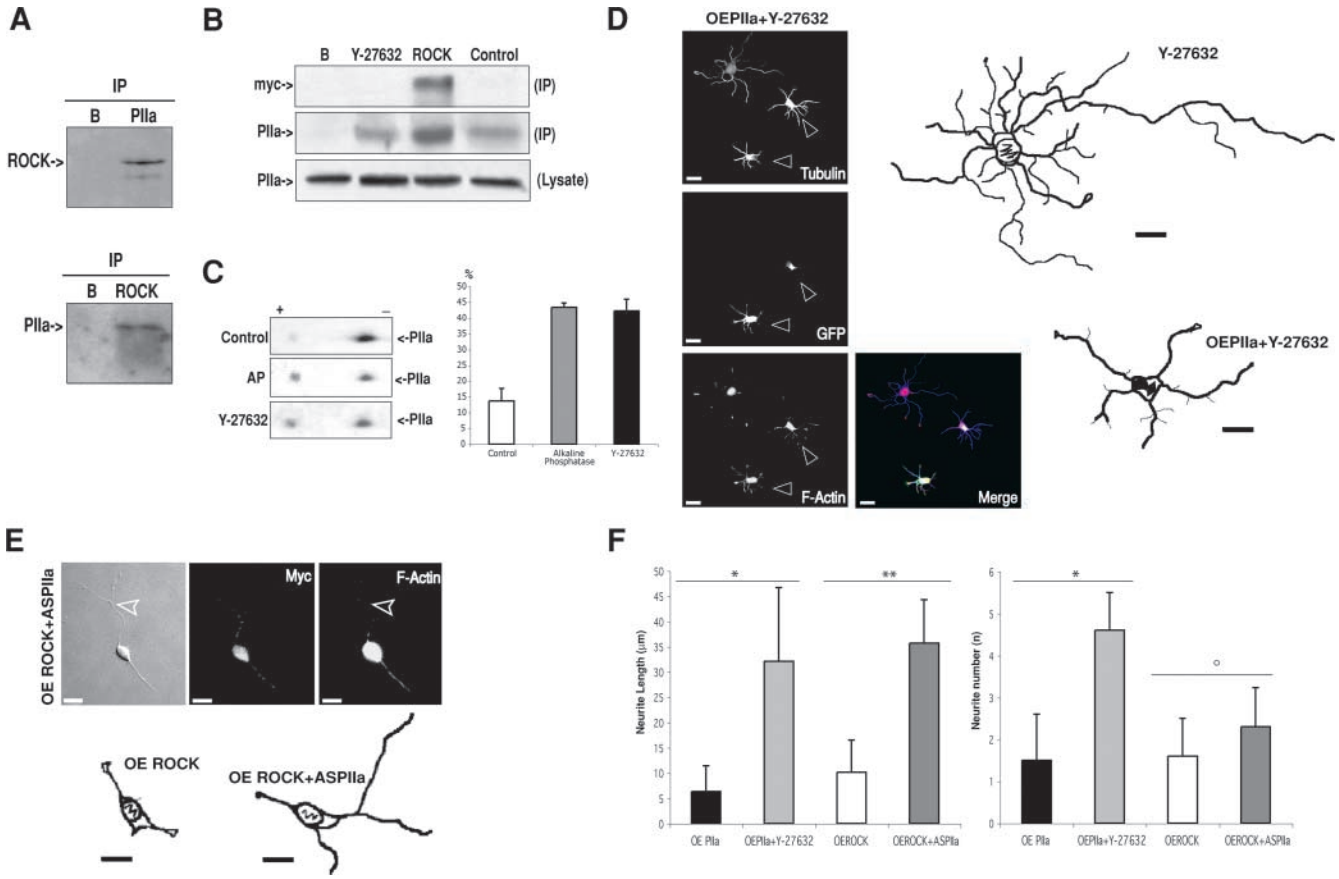

Figure 6. **ROCK physically and functionally interacts with PIIa.** (A) Brain cell homogenates immunoprecipitated with anti-PIIa antibody followed by blotting with anti-ROCK antibody (top) or immunoprecipitated with anti-ROCK antibody followed by blotting with anti-PIIa antibody (bottom). Both ROCK and PIIa are reciprocally immunoprecipitated. No signal is detected when protein G beads are incubated without antibodies (B). (B) Western blotting with the PIIa antibody of untransfected cells treated with the ROCK inhibitor (Y-27632, 6 h) or buffer-treated (control) cells, reveals that the amount of immunoprecipitated PIIa does not depend on the phosphorylation activity of ROCK (middle, PIIa, IP). Western blotting with the PIIa antibody of transfected (myc-ROCK) and un-transfected (control) cells, reveals that the amount of immunoprecipitated PIIa is higher in cells with higher levels of ROCK (middle, PIIa, IP). ROCK expression is detected with a myc-specific antibody (top, myc, IP). No PIIa signal is detected when extracts are incubated with beads without ROCK antibody (middle, PIIa, IP). To control for the presence and levels of PIIa, preimmunoprecipitation lysates were blotted with PIIa antibody (bottom, PIIa, lysate). (C) Western blots of 2D-SDS-PAGE samples from neuronal extracts blotted with anti-PIIa antibody. PIIa is present in two clearly distinguishable spots (control). The more negative form (+ to − labels the isoelectrical focusing direction) corresponds to a more phosphorylated form (AP-sensitive, histogram). Y-27632 (6 h) increases the percentage of dephosphorylated PIIa versus control (43% increase, histogram), whereas the more phosphorylated form is lower than in controls (histogram: only Δ% for the more dephosphorylated form is shown; data are mean + SD values; $n = 3$; $P < 0.001$ for AP and Y-27632 in comparison with control; 100% is the sum of both forms of PIIa). (D) Inhibition of ROCK activity (18 h) increases neurite sprouting (Y-27632 reconstruction and unmarked cells). This phenotype is significantly prevented by PIIa overexpression (OEPIIa + Y-27632 reconstruction and GFP-positive cells, arrowheads) and accompanied by an increase of the F-actin content. (E) ROCK overexpression induces a dramatic arrest of differentiation (Fig. 2 B and OE ROCK reconstruction). PIIa antisense on a ROCK overexpression background results in partial reversion of the ROCK phenotype, with longer neurites and reduced F-actin (arrowhead and OE ROCK + ASPIIa reconstruction). (F) Quantitative analysis indicates that overexpression of PIIa (OEPIIa, $n = 21$) causes an arrest in neurite budding and elongation. Inhibition of ROCK, in this experimental background (OEPIIa + Y-27632, $n = 22$), leads to a very significant recovery with neurites reaching control-like number and length, but not to the levels observed for ROCK inhibition alone (compare with Fig. 2 C). Overexpression of ROCK (OE ROCK, $n = 27$) inhibits neurite sprouting and extension. PIIa antisense in this case (OE ROCK + ASPIIa, $n = 26$) results in a partial phenotype rescue, as processes elongate further, but cells do not sprout more neurites. Data are mean + SD values. *, $P < 0.001$, OEPIIa + Y-27632 in comparison with OEPIIa; **, $P < 0.001$, OEROCK + ASPIIa in comparison with OEROCK; °, $P < 0.05$, OEROCK + ASPIIa in comparison with OEROCK. Bars, 10 µm.

chemical and functional experiments. First, we tested if both molecules interact physically. Indeed, ROCK and PIIa interact as observed by reciprocal co-immunoprecipitations (Fig. 6 A). Second, we determined if the intrinsic kinase activity of ROCK is important for complex formation. Extracts treated with Y-27632 do not display any change in the efficiency of PIIa immunoprecipitation by ROCK (Fig. 6 B), indicating that the kinase activity is not essential for PIIa binding. Finally, we assessed if the intracellular levels of ROCK influence complex formation. This is the case as ROCK overexpression increases the efficiency of PIIa recruitment (Fig. 6 B). Noticeably, ROCK does not immunoprecipitate profilin I (unpublished data), indicating that, at least in the very early steps of neuronal differentiation, the ROCK pathway is selective for the brain-specific form of profilin.

These results imply that ROCK interacts with PIIa in a stoichiometric fashion and suggest that its kinase activity is not essential for recruitment efficiency, though it might underlie the mechanism by which it regulates PIIa. To address this, we analyzed neuronal extracts in two-dimensional gels. In control conditions, PIIa is present in two distinguishable forms (Fig. 6 C, Control). One of these forms is more phosphorylated than the other because it is more negative in the isoelectric focusing direction and is reduced when extracts are previously treated with the phosphorylation inhibitor alkaline phosphatase (Fig. 6 C, AP and histogram). Significantly, extracts of cells treated with Y-27632 present an increase in the more dephosphorylated form of PIIa (Fig. 6 C, Y-27632 and histogram), similar to that observed with alkaline phosphatase (43%). These results indicate that ROCK regulates PIIa via its serine/threonine kinase activity.

To examine the functional relevance of these findings we asked whether the increased budding and extension of neurites, observed when ROCK is inactivated (Fig. 2 A), could be prevented by excess PIIa, which increases the concentration of ROCK–PIIa complexes. In fact, when we overexpressed PIIa-GFP and inhibited ROCK activity, cells were less differentiated than untransfected, ROCK-inhibited cells (Fig. 6 D and Fig. 2 A). At the same time, these cells were significantly more differentiated than PIIa overexpressing cells alone (Fig. 6 D and Fig. 3 D) and presented a reduction in F-actin content (Fig. 5 A), indicating that these neurons were sensitive to the absence of ROCK activity. Thus, the kinase activity of ROCK is essential to regulate the neuritogenic arrest effects of PIIa. To further substantiate this functional link, we tested whether reducing the pool of PIIa could, to any extent, rescue the effects of ROCK overexpression. Indeed, reduction of PIIa levels in ROCK overexpressing cells resulted in a milder ROCK phenotype (Fig. 6 E). No reversion on the ROCK phenotype was observed when PIIa missense oligonucleotides were added (unpublished data). Comparison of average neurite number and length between the aforementioned phenotypes (Fig. 6 F) further substantiates our conclusion that ROCK and PIIa interact functionally. Altogether, these results establish that PIIa is a major downstream target of ROCK during the initial steps of neuronal differentiation.

PIIa is a downstream effector of RhoA

Because ROCK and PIIa are functionally linked and ROCK is a main effector of RhoA, the activity of RhoA might be involved in the dynamics of ROCK–PIIa complex formation. To test this, we expressed constitutively active RhoA or we inhibited RhoA and analyzed the efficiency of ROCK–PIIa complex formation. Although in the case of constitutively active RhoA, ROCK recruits PIIa more efficiently, the reverse is observed when RhoA activity is decreased by C3 overexpression (Fig. 7 A). This suggests that RhoA activity is key to ROCK–PIIa complex formation. Previous work has shown that RhoA specifically activates the kinase activity of ROCK and is responsible for its direct recruitment to the membrane once it is activated (Leung et al., 1995; Matsui et al., 1996). Thus, inefficient complex formation and consequent lack of PIIa phosphorylation explains the phenotype induced by RhoA inactivation (Fig. 1 B). Conversely, RhoA activation favors ROCK–PIIa interaction and PIIa phosphorylation, and this would explain the neuritogenic arrest caused by V14RhoA overexpression (Fig. 1 A).

Consistent with RhoA acting as an upstream regulator of PIIa, coexpression of RhoA inactivating HA-C3 and PIIa-GFP precludes the previously observed effects of RhoA inactivation (Fig. 7 B and Fig. 1 A). In parallel, cotransfected cells exhibit a milder PIIa phenotype that greatly resembles control hippocampal neurons (Fig. 7 B). In addition, reduction of PIIa intracellular levels precludes, in part, the effect of constitutively active RhoA expression (Fig. 7 C). Partially rescued V14RhoA overexpressing cells were able to extend neurites, although there was no improvement in the number of sprouting neurites (Fig. 7 C and Fig. 1 A). No phenotypic reversion was detected with missense oligonucleotides (unpublished data). Comparative statistical analysis of the RhoA-related experiments (Fig. 7 D) confirms the conclusions drawn from the morphological analysis. Together, these results demonstrate that PIIa is a downstream effector of RhoA, and that PIIa-directed actin stability regulation is under the control of RhoA/ROCK.

PIIa regulation by RhoA and ROCK can be modulated by extracellular physiological stimuli

To assess if the proposed molecular mechanism has potential relevance in situ, we analyzed whether the players responsible for ROCK–PIIa complex formation (RhoA) and for PIIa phosphorylation (ROCK) are under the influence of known physiological stimuli.

Thus, we first investigated if growth-promoting soluble stimuli have the capacity to accelerate differentiation in our system. Indeed, growth factors known to favor neurite extension in vivo, such as neurotrophin 3 (NT-3), brain-derived neurotrophic factor (BDNF), and NGF, induce, at early stages of hippocampal neuron differentiation, an increase in process length and number (Fig. 8, A, Control and C). However, neurons overexpressing V14RhoA or ROCK are highly refractory to NT-3, BDNF, or NGF (Fig. 8, A and C). On the one hand, these results indicate that these factors act through RhoA, not only during later stages of differentiation (Yamashita et al., 1999) but also during neuritogenesis. On the other hand, they suggest that at early differentiation stages positive stimuli have the capacity to induce RhoA inactivation and consequent loss of ROCK–PIIa complex formation efficiency. Indeed, the neuritogenic effects of all three neurotrophins can be prevented by PIIa overexpression (Fig. 8 A).

In addition, we tested if substrate-bound ligands also display the capacity to shape the RhoA–ROCK-PIIa neuritogenic response. Hippocampal neurons plated in the in vivo growth-favoring substratum laminin show enhanced neurite formation and elongation (Fig. 8, B and C). In contrast, cells plated in collagen, a poorly permissive support layer for hippocampal neurons, show arrested sprouting and elongation, compared with a poly-L-lysine control (Fig. 8, B and C). Although laminin has been shown to inactivate RhoA (Leeuwen et al., 1997; Liu et al., 2002),

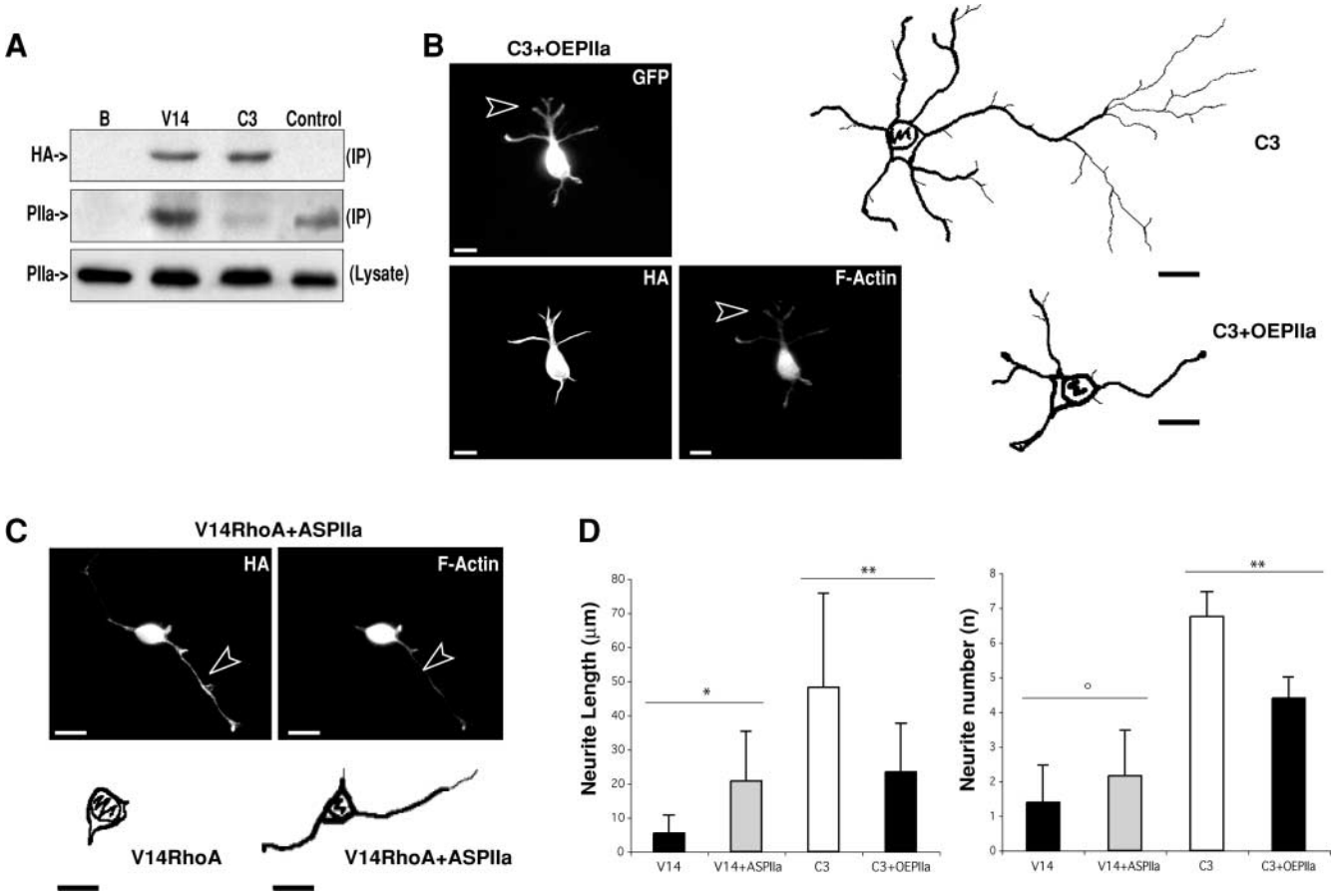

Figure 7. **PIIa is a downstream effector of RhoA.** (A) ROCK immunoprecipitation of cell extracts overexpressing constitutively active RhoA (V14) or inactive Rho (C3, 24 h), followed by Western blotting with PIIa antibody. V14RhoA increases the amount of PIIa immunoprecipitated by ROCK (middle, PIIa, IP), whereas C3 reduces the amount of PIIa immunoprecipitated by ROCK (middle, PIIa, IP). V14RhoA and C3 expression is detected with an HA-specific antibody (top, HA, IP). No signal is detected (B) when extracts are precipitated without ROCK antibody (middle, PIIa, IP). To control for the presence and levels of PIIa, preimmunoprecipitation lysates were blotted with PIIa antibody (bottom, PIIa, lysate). (B) C3 expression (24 h) enhances neurite sprouting (Fig. 1 A and C3 reconstruction). Co-transfection with PIIa-GFP (C3 + OEPIIa, 24 h) prevents the increased neurite sprouting and elongation characteristic of C3 expression (C3 + OEPIIa reconstruction) and favors actin polymerization at the distal fractions of budding neurites (arrowhead). Conversely, the overall F-actin content is reduced in comparison with PIIa overexpression alone (compare with Fig. 5 A). (C) Constitutively active RhoA induces a differentiation-arrested phenotype (Fig. 1 A and V14RhoA reconstruction). Reduction of PIIa levels partially reverts this arrest (V14RhoA + ASPIIa reconstruction); these cells show a less polymerized actin cytoskeleton, namely along elongated processes (arrowhead) but do not sprout more neurites (compare with Fig. 1 B). (D) Statistical analysis shows that PIIa antisense (V14 + ASPIIa, $n = 28$) incompletely rescues the V14-induced (V14, $n = 22$) phenotype as neurons extend longer neurites, but there is no detectable change in neurite number. On the contrary, compared with single HA-C3 transfection (C3, $n = 22$), co-transfection of HA-C3 and PIIa-GFP (C3 + OEPIIa, $n = 24$) results in a decrease of neurite number and length. Data are mean + SD values. *, $P < 0.001$, V14 + ASPIIa in comparison with V14; **, $P < 0.001$, C3 + OEPIIa in comparison with C3; °, $P < 0.05$, V14 + ASPIIa in comparison with V14. Bars, 10 μm.

collagen has been found to activate RhoA in other cell types (Schoenwaelder et al., 2002). Supporting our findings, recently plated neurons with excess V14RhoA or ROCK are highly refractory to laminin (Fig. 8, B and C). On the other hand, the collagen effect on sprouting was less obvious in cells expressing C3 or in cells treated with Y-27632 (Fig. 8, B and C). Furthermore, PIIa overexpressing cells prevent the positive effects of laminin, whereas reduction of PIIa levels in collagen-plated cells partly reverts the arrest stimulus (Fig. 8, B and C). This last series of results show that extracellular stimuli can induce modifications in the activity of the RhoA–ROCK pathway by allowing an adaptative regulation of PIIa function and point out the physiological relevance of the findings described here.

Discussion

In this work, we show that the activity of RhoA and its downstream effector ROCK control initial sprouting: activation leads to neuritogenic arrest, whereas inactivation accelerates neuritogenesis. RhoA and ROCK have been described as negative regulators of neuritic growth in later differentiation stages (Introduction). Our results are consistent with such a role, and favor the emerging view that similar molecular mechanisms can be used throughout the entire neuronal morphogenesis program (Da Silva and Dotti, 2002; Luo, 2002).

The observed RhoA and ROCK activity phenotypes are accompanied by changes in F-actin content, suggesting that downstream actin-related proteins are implicated in neuritogenesis. We demonstrate that the brain-specific protein PIIa

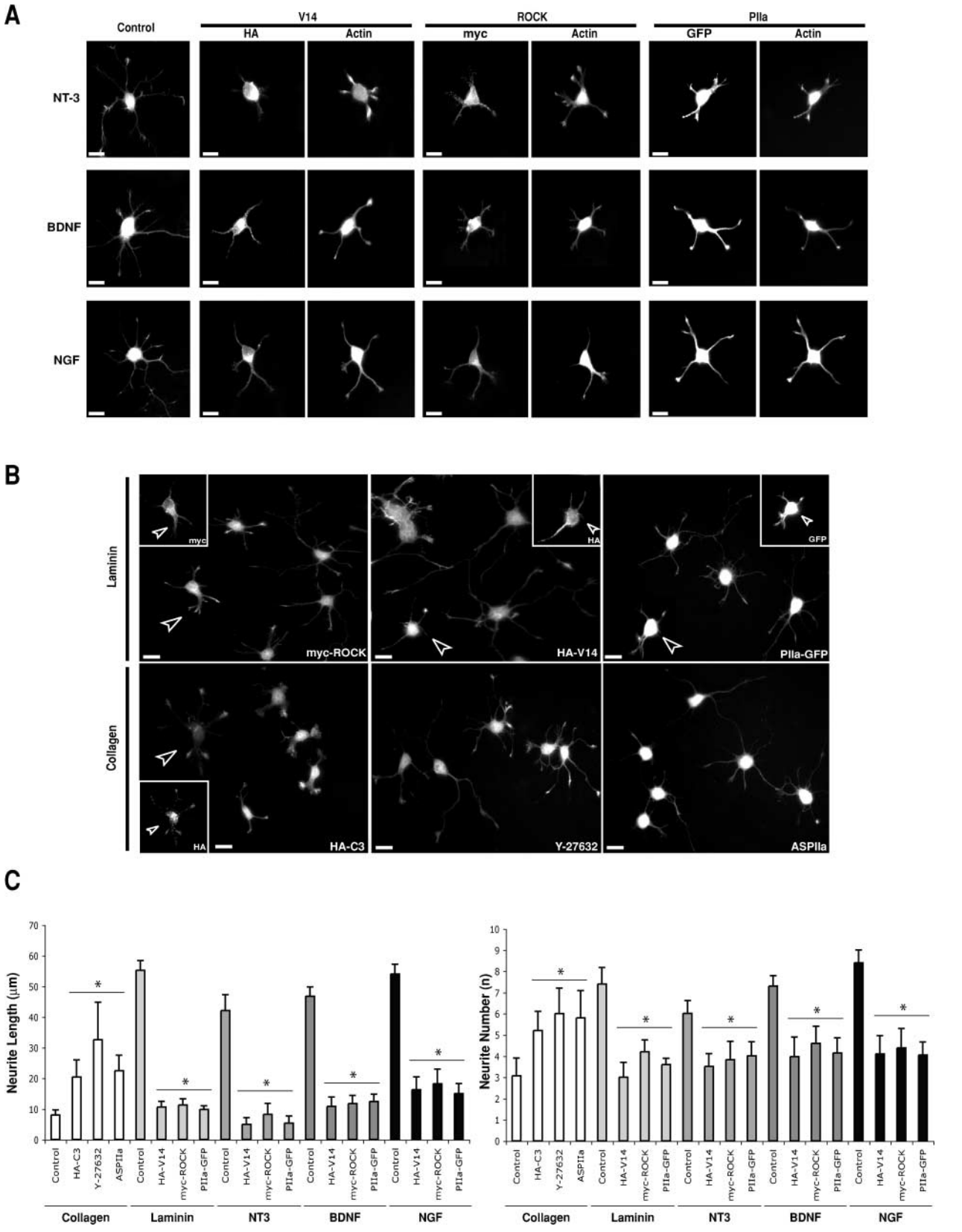

Figure 8. **Extracellular stimuli mimic the RhoA/ROCK modulation of PIIa.** (A) Neurons treated with different neurotrophins (NT-3, BDNF or NGF) at 50 ng/ml sprout numerous long neurites (Control) compared with untreated cells (compare with Fig. 1 A). Cells treated and transfected with HA-V14RhoA, myc-ROCK, or PIIa-GFP are refractory to these growth-promoting effects. (B) Neurons overexpressing ROCK (arrowhead and myc inset in the myc-ROCK panel), constitutively active RhoA (arrowhead and HA inset in the HA-V14 panel), or PIIa (arrowhead and GFP inset in the PIIa-GFP panel) interfere with the effect of the growth-promoting substratum laminin (unmarked cells in the respective panels). Cells either overexpressing inactive Rho (arrowhead and inset in the HA-C3 [24 h] panel), or treated with Y-27632 (18 h) or with low PIIa levels

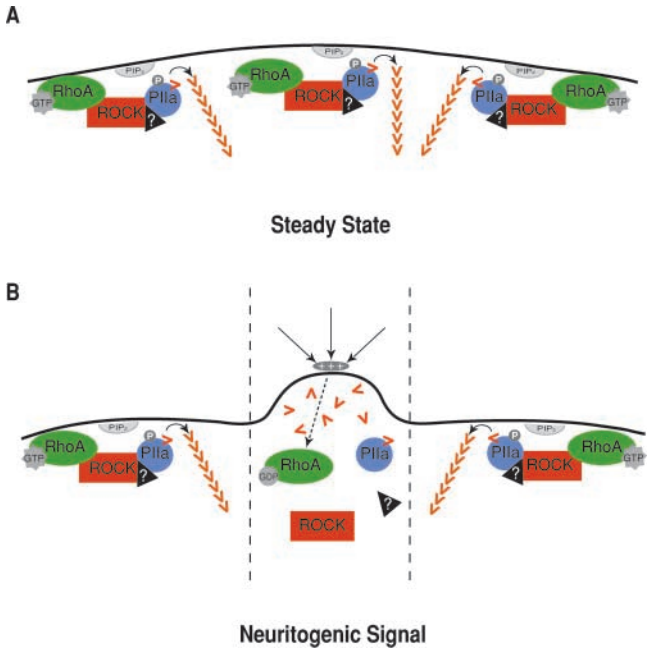

Figure 9. **Proposed involvement of RhoA/ROCK/PIIa in the regulation of mammalian neuritogenesis.** (A) At steady state, before neuritogenesis ensues, cellular shape is kept as the submembranous actin cytoskeleton is evenly stabilized (external signals are not depicted for simplicity). This depends, at least in part, on the dominance of the RhoA–ROCK–PIIa pathway described here, where RhoA recruits and activates ROCK which, in turn, phosphorylates PIIa. Importantly, in recently dissociated neurons most of the PIIa is phosphorylated (Fig. 6 C). The neuritogenic–arrest complex might comprise other yet unidentified proteins that influence ROCK–PIIa complex formation, regulate PIP_2 function, and/or bring to close vicinity other actin-related proteins (such as cofilin or myosin). (B) Upon contact of a segment of the membrane with a growth-positive signal, RhoA is inactivated and locally dissociates from the membrane. This reduces the interaction between ROCK and PIIa and decreases phosphorylated PIIa (and probably reduces local accumulation of PIP_2). This translates into a very localized shift in the local F/G actin ratio, favoring the monomeric form leading to actin instability and sprout formation. Localization of the incoming signal, whether qualitative or quantitative (gradient), would explain how a ubiquitously distributed intracellular pathway can be modulated to allow neuritogenesis at a particular spot of the cell sphere (between dashed lines).

is directly involved in neuritogenesis, as PIIa deficiency induces actin depolymerization and multiple sprouting, whereas overexpression of PIIa hinders neuritogenesis due to hyperstabilization of the actin cytoskeleton. These results indicate that PIIa is required to modulate actin polymerization, thus hindering or facilitating neurite budding. This is supported by recent studies in yeast, where profilin plays an important role in actin cable formation (Evangelista et al., 2002; Sagot et al., 2002). Noticeably, there is an obvious resemblance between yeast budding and neurite sprouting from an initially spherical soma (Da Silva and Dotti, 2002). However, our results contrast with findings in *Drosophila*, where *chickadee* favors neurite extension (Wills et al., 1999). It is possible that different tissue-specific isoforms allow mammalian cells a finer control of the actin system.

PIIa overexpression and deficiency, respectively, phenocopy RhoA/ROCK gain and loss of function. This reflects a true molecular interaction between ROCK and PIIa because: (a) both proteins can be reciprocally coimmunoprecipitated, as suggested by affinity chromatography (Witke et al., 1998); (b) ROCK recruits PIIa in a stoichiometric fashion; (c) the kinase activity of ROCK is necessary for PIIa phosphorylation, probably in a PIP_2-dependent manner because PIIa binds PIP_2 (Lambrechts et al., 2000) and ROCK controls its intracellular availability (Yamamoto et al., 2001); and (d) ROCK activation/inactivation phenotypes can be prevented by changing intracellular PIIa levels, and thus its availability to associate with ROCK. Because rescues are not complete, alternative ROCK downstream effectors might also play a role in neuritogenesis. One of these could be LIMK-1, a target known to be important in the later stages of axon outgrowth (Bito et al., 2000). However, prevention of ROCK inactivation effects through manipulation of LIMK-1 is less robust (Bito et al., 2000), indicating that PIIa is a key actin-binding protein, at least during the first stages of differentiation.

Our work also reveals that RhoA activity regulates the formation of the ROCK–PIIa complex. RhoA is the upstream regulator of ROCK and target of various physiological stimuli influencing neuronal differentiation (Introduction). That loss of RhoA activity can rescue PIIa overexpression and that PIIa reduction reverts the enhanced RhoA activity phenotype illustrates the functional relevance of our findings. Such significant but incomplete morphological reversions hint at potential synergies between the effects of RhoA on PIIa and on other actin stabilization targets, such as myosin. ROCK phosphorylates myosin light chain phosphatase to regulate the formation of actin fibers (for review see Tapon and Hall, 1997). It is tempting to speculate that myosin-related proteins might be members of the ROCK–PIIa complex, where both the regulatory kinase and an actin monomer-binding protein are present.

Neurons have different actin-binding proteins; which and how each is activated depends on the momentary properties of the extracellular milieu that activate specific intracellular pathways. Consistent with this idea, stimuli known to promote growth via inactivation of RhoA were not able to do so in the presence of excess ROCK or PIIa, whereas stimuli that activate RhoA could not prevent neurite formation in cells with inactivated ROCK or reduced levels of PIIa.

(ASPIIa) are able to differentiate in the presence of a growth unfavorable collagen-rich substratum that normally induces reduced sprouting and elongation (exemplified by unmarked cells in the HA-C3 panel). Transfected cells in individual insets are either labeled with specific antibodies against myc (inset in myc-ROCK panel) and HA (insets in HA-V14 and HA-C3 panels) or detected by GFP fluorescence (inset in PIIa-GFP panel). (C) Quantitative analysis of experiments shown in A and B. Measurements of neurite length and number shows that the effects of different extracellular stimuli on neurite sprouting and initial elongation can be modulated by modifying the activity of RhoA, ROCK and PIIa. The same number of cells was used for each experimental condition tested for every external stimuli: NT-3, $n = 31$; BDNF, $n = 29$; NGF, $n = 34$; Laminin, $n = 23$; and Collagen, $n = 18$. Data are mean + SD values; *, $P < 0.001$, in comparison with respective controls presented with same extracellular stimuli (grouped by lower horizontal bar). Cells were labeled with phalloidin. Bars, 10 μm.

Previous work on neuritogenesis has largely relied on derived cell lines (Hirose et al., 1998), where ROCK is known to impair process extension usually induced by in vitro manipulations such as serum starvation. By analyzing the time span in which mammalian neurons naturally sprout neurites (that later will become specialized axons and dendrites), we now show that ROCK, together with RhoA, PIIa, and actin, is part of an important mechanism, in-built in the differentiation program of hippocampal neurons and regulated by known in vivo physiological stimuli. Such mechanism elucidates how one cell can respond to simultaneous, neighboring signals that favor or discourage actin polymerization. This, in turn, would determine if a sprout forms at a given location of the round, undeveloped neuron (Fig. 9). It is tempting to hypothesize that RhoA/ROCK/PIIa–mediated events may also be key for the different architectural modifications occurring at later stages of neuronal differentiation, such as axon formation and elongation.

Materials and Methods

Cell culture

Primary cultures of rat embryo hippocampal neurons were prepared as described previously (Goslin and Banker, 1991). For biochemical analysis, cells were plated onto dishes coated with 0.1 mg/ml poly-L-lysine (PLL) and for morphological studies onto PLL-, laminin- (2 μg/ml), or collagen-treated (25 μg/ml) glass coverslips. Primary cultures of PII+/− and PII−/− mice were prepared following the same protocol. All times (hours) referred to are after seeding. Cytochalasin D was used at 1 μM (Sigma-Aldrich) and Y-27632 at 37 nmol/ml (BIOMOL Research Laboratories, Inc.).

Transient transfections

Neurons in suspension were electroporated (20 μg DNA/400 μl suspension) using a GenePulser (Bio-Rad Laboratories) set at 250 V, 250 μF, and 200 Ω. Cells were analyzed at 24 h in culture. Where stated, lipofection was used (Effectene; QIAGEN). The following plasmids were used: pPIIa-EGFP (termed PIIa-GFP), null GFP vector pEGFP-N1 (CLONTECH Laboratories, Inc.), pIRES-neo/Sendai/PIIa (Di Nardo et al., 2000), untagged pIRES-neo/PIIa (Di Nardo et al., 2000), empty vector pIRES-neo (CLONTECH Laboratories, Inc.), pRc/HA-V14 and pRc/HA-C3 (a gift from J. Settleman, Massachusetts General Hospital, Charlestown, MA), empty vector pRc/HA (CLONTECH Laboratories, Inc.), and pEF-Bos-myc/ROCK (a gift from K. Kaibuchi, Nagoya University, Nagoya, Japan).

Antisense treatments

Treatments were performed using antisense (5′-CCACGTAGCTCTGC-CAACCGGCCAT-3′) and control 4-missense (5′-CCACcTAGCaCTGC-CtACCGcCCAT-3′; lowercase for missense nucleotides) Morpholino oligonucleotides (Gene Tools). These, prepaired with partially complementary DNA, were incubated with delivery solution (EPEI) for 30 min and added 3 h after seeding. Final Morpholino and EPEI concentrations were 0.25 nmol/ml and 0.03 nmol/ml, respectively. Cells were analyzed after 24 h in culture.

Western blotting, 2D gels, and immunoprecipitation

Neuronal extracts were loaded onto SDS-PAGE gels (equal protein amounts following spectrophotometric determination) and proteins were transferred to nitrocellulose filters. These were then incubated with rabbit polyclonal PIIa-specific antibody (Witke et al., 2001), mouse monoclonal α-tubulin–specific antibody (N536; Amersham Biosciences), mouse monoclonal mannosidase2-specific antibody (a gift from G. Griffiths, EMBL, Heidelberg, Germany), and with rabbit polyclonal PI-specific antibody (Witke et al., 2001). After secondary antibody incubation, nitrocellulose membranes were developed using an ECL system (Amersham Biosciences). Quantification was performed by densitometry of autoradiograms, using NIH Image 1.62 software and Microsoft Excel v. X. Quantified Western blots were plotted for PIIa expression levels in arbitrary units (a.u.) of optical density, normalized against the unrelated Golgi protein mannosidase-2 in the population. In all cases, quantification was based on four independent experiments. 2D gel separation of neuronal extracts was followed by the same Western blotting procedure. For immunoprecipitations, extracts were obtained with lysis buffer (1% Triton X-100, 100 mM NaCl, 2 mM EDTA, 10 mM Tris/HCl, pH 7.5, and protease inhibitors) and incubated at 4°C overnight with anti-PIIa or anti–ROCK-II (clone 21; BD Biosciences) antibodies coupled to protein G–Sepharose beads (Roche). Beads without antibodies incubated with homogenates were used as controls. Samples were analyzed following the same Western Blotting protocol.

Morphological analysis

Neurons were analyzed by immunofluorescence using the following antibodies: anti–mouse α-tubulin antibody, mouse monoclonal 12CA5 anti-HA antibody (Boehringer), mouse monoclonal 9E10 anti-myc antibody (American Type Culture Collection), and rabbit polyclonal anti-PIIa antibody. F-actin was detected with Alexa 568–conjugated phalloidin (Molecular Probes). Alexa-conjugated secondary antibodies (Molecular Probes) were used. Cells were observed with a microscope equipped with 40×, 63×, and 100× objectives (model DMIRE2; Leica), and images were captured using Qfluoro software (Leica). Neurite length and number were measured using this software, by two observers, from at least three independent experiments. Obtained values were exported to Excel v. X for statistical analysis. Student's *t* tests were based on our results' two-tailed distribution and two-sample unequal variance.

F/G-actin ratios

Determination of F- and G-actin fluorescence, labeled with Alexa 568 phalloidin and Alexa 488 DNaseI (Molecular Probes), respectively, was done with the ProbeMeter plug-in of the Qfluoro software. Images from F- and G-actin channels were captured and merged. A user-determined 5 × 5-pixel area was placed at 10 different points along each neurite (control, $n = 90$; antisense, $n = 88$; overexpression, $n = 35$), and the percentage of signal from each channel was calculated by the software against the unmodified background. The results obtained were statistically analyzed with Excel v. X.

Morphological reconstructions

For the different experimental backgrounds, phase-contrast images of individual cells were obtained. Preparation of camera lucida drawings for each particular image ensued, after which a montage of camera lucida reconstructions was produced. This resulted in drawings of average cells, each representative of individual experimental perturbations and respective controls. Thicker lines depicted thicker processes and the cell body, whereas thinner processes were drawn with increasingly finer lines. Degree of branching was represented by a variable number of stemming processes.

We thank Bianca Hellias and Etienne Cassin for technical assistance and Jose Abad-Rodriguez, Maria Dolores Ledesma, and Vanessa Schubert for helpful suggestions.

J.S. Da Silva is supported by an FCT/PRAXIS XXI scholarship (Portuguese Ministry of Science and Technology).

Submitted: 3 April 2003
Accepted: 14 August 2003

References

Arber, S., F.A. Barbayannis, H. Hanser, C. Schneider, C.A. Stanyon, O. Bernard, and P. Caroni. 1998. Regulation of actin dynamics through phosphorylation of cofilin by LIM-kinase. *Nature.* 393:805–809.

Bamburg, J.R. 1999. Proteins of the ADF/cofilin family: essential regulators of actin dynamics. *Annu. Rev. Cell Dev. Biol.* 15:185–230.

Baum, P.D., and G. Garriga. 1997. Neuronal migrations and axon fasciculation are disrupted in ina-1 integrin mutants. *Neuron.* 19:51–62.

Billuart, P., C.G. Winter, A. Maresh, X. Zhao, and L. Luo. 2001. Regulating axon branch stability: the role of p190 RhoGAP in repressing a retraction signaling pathway. *Cell.* 107:195–207.

Bito, H., T. Furuyashiki, H. Ishihara, Y. Shibasaki, K. Ohashi, K. Mizuno, M. Maekawa, T. Ishizaki, and S. Narumiya. 2000. A critical role for a Rho-associated kinase, p160ROCK, in determining axon outgrowth in mammalian CNS neurons. *Neuron.* 26:431–441.

Bradke, F., and C.G. Dotti. 1999. The role of local actin instability in axon formation. *Science.* 283:1931–1934.

Da Silva, J.S., and C.G. Dotti. 2002. Breaking the neuronal sphere: regulation of the actin cytoskeleton in neuritogenesis. *Nat. Rev. Neurosci.* 3:694–704.

Di Nardo, A., R. Gareus, D. Kwiatkowski, and W. Witke. 2000. Alternative splicing of the mouse profilin II gene generates functionally different profilin isoforms. *J. Cell Sci.* 113:3795–3803.

Dotti, C.G., C.A. Sullivan, and G.A. Banker. 1988. The establishment of polarity by hippocampal neurons in culture. *J. Neurosci.* 8:1454–1468.

Evangelista, M., D. Pruyne, D.C. Amberg, C. Boone, and A. Bretscher. 2002. Formins direct Arp2/3-independent actin filament assembly to polarize cell growth in yeast. *Nat. Cell Biol.* 4:32–41.

Gleeson, J.G., and C.A. Walsh. 2000. Neuronal migration disorders: from genetic diseases to developmental mechanisms. *Trends Neurosci.* 23:352–359.

Goslin, K., and G. Banker. 1991. Rat hippocampal neurons in low-density culture. *In* Culturin Nerve Cells. K. Goslin and G. Banker, editors. Massachusetts Institute of Technology Press, Cambridge, MA. 251–281.

Haarer, B.K., S.H. Lillie, A.E. Adams, V. Magdolen, W. Bandlow, and S.S. Brown. 1990. Purification of profilin from *Saccharomyces cerevisiae* and analysis of profilin-deficient cells. *J. Cell Biol.* 110:105–114.

Hatten, M.E. 1999. Central nervous system neuronal migration. *Annu. Rev. Neurosci.* 22:511–539.

Haugwitz, M., A.A. Noegel, J. Karakesisoglou, and M. Schleicher. 1994. *Dictyostelium amoebae* that lack G-actin-sequestering profilins show defects in F-actin content, cytokinesis, and development. *Cell.* 79:303–314.

Hirose, M., T. Ishizaki, N. Watanabe, M. Uehata, O. Kranenburg, W.H. Moolenaar, F. Matsumura, M. Maekawa, H. Bito, and S. Narumiya. 1998. Molecular dissection of the Rho-associated protein kinase (p160ROCK)–regulated neurite remodeling in neuroblastoma N1E-115 cells. *J. Cell Biol.* 141:1625–1636.

Hu, E., Z. Chen, T. Fredrickson, and Y. Zhu. 2001. Molecular cloning and characterization of profilin-3: a novel cytoskeleton-associated gene expressed in rat kidney and testes. *Exp. Nephrol.* 9:265–274.

Ishizaki, T., M. Uehata, I. Tamechika, J. Keel, K. Nonomura, M. Maekawa, and S. Narumiya. 2000. Pharmacological properties of Y-27632, a specific inhibitor of rho-associated kinases. *Mol. Pharmacol.* 57:976–983.

Jalink, K., T. Eichholtz, F.R. Postma, E.J. van Corven, and W.H. Moolenaar. 1993. Lysophosphatidic acid induces neuronal shape changes via a novel, receptor-mediated signaling pathway: similarity to thrombin action. *Cell Growth Differ.* 4:247–255.

Jalink, K., E.J. van Corven, T. Hengeveld, N. Morii, S. Narumiya, and W.H. Moolenaar. 1994. Inhibition of lysophosphatidate- and thrombin-induced neurite retraction and neuronal cell rounding by ADP ribosylation of the small GTP-binding protein Rho. *J. Cell Biol.* 126:801–810.

Kaibuchi, K., S. Kuroda, and M. Amano. 1999. Regulation of the cytoskeleton and cell adhesion by the Rho family GTPases in mammalian cells. *Annu. Rev. Biochem.* 68:459–486.

Kozma, R., S. Sarner, S. Ahmed, and L. Lim. 1997. Rho family GTPases and neuronal growth cone remodelling: relationship between increased complexity induced by Cdc42Hs, Rac1, and acetylcholine and collapse induced by RhoA and lysophosphatidic acid. *Mol. Cell. Biol.* 17:1201–1211.

Lambrechts, A., A. Braun, V. Jonckheere, A. Aszodi, L.M. Lanier, J. Robbens, I. Van Colen, J. Vandekerckhove, R. Fassler, and C. Ampe. 2000. Profilin II is alternatively spliced, resulting in profilin isoforms that are differentially expressed and have distinct biochemical properties. *Mol. Cell. Biol.* 20:8209–8219.

Leeuwen, F.N., H.E. Kain, R.A. Kammen, F. Michiels, O.W. Kranenburg, and J.G. Collard. 1997. The guanine nucleotide exchange factor Tiam1 affects neuronal morphology; opposing roles for the small GTPases Rac and Rho. *J. Cell Biol.* 139:797–807.

Leung, T., E. Manser, L. Tan, and L. Lim. 1995. A novel serine/threonine kinase binding the Ras-related RhoA GTPase which translocates the kinase to peripheral membranes. *J. Biol. Chem.* 270:29051–29054.

Liu, R.Y., R.S. Schmid, W.D. Snider, and P.F. Maness. 2002. NGF enhances sensory axon growth induced by laminin but not by the L1 cell adhesion molecule. *Mol. Cell. Neurosci.* 20:2–12.

Luo, L. 2000. Rho GTPases in neuronal morphogenesis. *Nat. Rev. Neurosci.* 1:173–180.

Luo, L. 2002. Actin cytoskeleton regulation in neuronal morphogenesis and structural plasticity. *Annu. Rev. Cell Dev. Biol.* 18:601–635.

Maekawa, M., T. Ishizaki, S. Boku, N. Watanabe, A. Fujita, A. Iwamatsu, T. Obinata, K. Ohashi, K. Mizuno, and S. Narumiya. 1999. Signaling from Rho to the actin cytoskeleton through protein kinases ROCK and LIM-kinase. *Science.* 285:895–898.

Matsui, T., M. Amano, T. Yamamoto, K. Chihara, M. Nakafuku, M. Ito, T. Nakano, K. Okawa, A. Iwamatsu, and K. Kaibuchi. 1996. Rho-associated kinase, a novel serine/threonine kinase, as a putative target for small GTP binding protein Rho. *EMBO J.* 15:2208–2216.

Nakagawa, O., K. Fujisawa, T. Ishizaki, Y. Saito, K. Nakao, and S. Narumiya. 1996. ROCK-I and ROCK-II, two isoforms of Rho-associated coiled-coil forming protein serine/threonine kinase in mice. *FEBS Lett.* 392:189–193.

Nakayama, A.Y., M.B. Harms, and L. Luo. 2000. Small GTPases Rac and Rho in the maintenance of dendritic spines and branches in hippocampal pyramidal neurons. *J. Neurosci.* 20:5329–5338.

Sagot, I., A.A. Rodal, J. Moseley, B.L. Goode, and D. Pellman. 2002. An actin nucleation mechanism mediated by Bni1 and profilin. *Nat. Cell Biol.* 4:626–631.

Schoenwaelder, S.M., S.C. Hughan, K. Boniface, S. Fernando, M. Holdsworth, P.E. Thompson, H.H. Salem, and S.P. Jackson. 2002. RhoA sustains integrin alpha IIbbeta 3 adhesion contacts under high shear. *J. Biol. Chem.* 277:14738–14746.

Sekine, A., M. Fujiwara, and S. Narumiya. 1989. Asparagine residue in the rho gene product is the modification site for botulinum ADP-ribosyltransferase. *J. Biol. Chem.* 264:8602–8605.

Selden, L.A., H.J. Kinosian, J.E. Estes, and L.C. Gershman. 1999. Impact of profilin on actin-bound nucleotide exchange and actin polymerization dynamics. *Biochemistry.* 38:2769–2778.

Summerton, J., D. Stein, S.B. Huang, P. Matthews, D. Weller, and M. Partridge. 1997. Morpholino and phosphorothioate antisense oligomers compared in cell- free and in-cell systems. *Antisense Nucleic Acid Drug Dev.* 7:63–70.

Tapon, N., and A. Hall. 1997. Rho, Rac and Cdc42 GTPases regulate the organization of the actin cytoskeleton. *Curr. Opin. Cell Biol.* 9:86–92.

Verheyen, E.M., and L. Cooley. 1994. Profilin mutations disrupt multiple actin-dependent processes during *Drosophila* development. *Development.* 120:717–728.

Wills, Z., L. Marr, K. Zinn, C.S. Goodman, and D. Van Vactor. 1999. Profilin and the Abl tyrosine kinase are required for motor axon outgrowth in the *Drosophila* embryo. *Neuron.* 22:291–299.

Witke, W., A.V. Podtelejnikov, A. Di Nardo, J.D. Sutherland, C.B. Gurniak, C. Dotti, and M. Mann. 1998. In mouse brain profilin I and profilin II associate with regulators of the endocytic pathway and actin assembly. *EMBO J.* 17:967–976.

Witke, W., J.D. Sutherland, A. Sharpe, M. Arai, and D.J. Kwiatkowski. 2001. Profilin I is essential for cell survival and cell division in early mouse development. *Proc. Natl. Acad. Sci. USA.* 98:3832–3836.

Wolven, A.K., L.D. Belmont, N.M. Mahoney, S.C. Almo, and D.G. Drubin. 2000. In vivo importance of actin nucleotide exchange catalyzed by profilin. *J. Cell Biol.* 150:895–904.

Yamamoto, M., D.H. Hilgemann, S. Feng, H. Bito, H. Ishihara, Y. Shibasaki, and H.L. Yin. 2001. Phosphatidylinositol 4,5-bisphosphate induces actin stress-fiber formation and inhibits membrane ruffling in CV1 cells. *J. Cell Biol.* 152:867–876.

Yamashita, T., K.L. Tucker, and Y.A. Barde. 1999. Neurotrophin binding to the p75 receptor modulates Rho activity and axonal outgrowth. *Neuron.* 24:585–593.